Including mixed layer convection when determining air-sea CO_2 transfer velocity

Anna Rutgersson, Ann-Sofi Smedman and Erik Sahlée

Department of Earth Sciences, Uppsala University, Uppsala, Sweden,
E-mail: anna.rutgersson@met.uu.se

Abstract. Using measurements made at the Östergarnsholm field station in the Baltic Sea it was previously shown that the CO_2 transfer velocity is a function not only of wind speed, but also of the mixed-layer depth of the water and, to a lesser degree, of the stratification of the atmosphere. The transfer velocity is significantly enhanced by a large mixed-layer depth, the enhancement increasing as the surface cooling increases. The impact of mixed layer depth is expressed by the convective velocity scale of the water (analogous to atmospheric convective scaling). The enhancement due to convection can be added to the traditional transfer velocity. An alternative method suggested here is to include mixed layer convection as an additional resistance in parallel with other processes acting to disturb the molecular sublayer. This additional resistance is introduced in the NOAA-COARE algorithm, showing good agreement with measured data.

Key Words: Air-sea exchange, Transfer velocity parameterization, CO_2 exchange, Eddy-correlation measurements, water-side convection

1. Introduction

The ocean is a sink for a large fraction of the anthropogenically produced CO_2. For full understanding of the global carbon cycle it is crucial to understand gas exchange across the air-sea interface, as it is an important component of global climate dynamics. Many measurements of oceanic CO_2 have been made in recent decades, but quantification of the total oceanic uptake and, in particular, the regional distribution of the oceanic uptake is still uncertain (Siegenthaler and Sarmiento 1993; IPCC, 2007; Takahashi *et al*. 2002).

The exchange of CO_2 between ocean and atmosphere is controlled by the air-sea difference in CO_2 partial pressure (ΔpCO_2) at the surface and by the efficiency of the transfer processes. The partial pressure at the water surface is controlled by biological, chemical, and physical processes in the water. The efficiency of the transfer processes is determined by the resistance to the transfer in the atmosphere and the ocean. The CO_2 diffusivity is much greater in the atmosphere than in water and the largest resistance to CO_2 transfer is due to molecular diffusion and turbulent mixing in the aqueous boundary layer. It is generally agreed that the molecular diffusion layer is dominating and processes disturbing this layer controls the transfer. Most investigations describe the transfer efficiency in terms of transfer velocity. Traditional estimates of air-sea exchange use relatively simple empirical wind-speed-dependent expressions for the transfer velocity (Liss and Merlivat, 1986; Wanninkhof, 1992; Wanninkhof *et al.* 2009). There are, however, several other physical processes contributing to air-sea transfer, including microwave breaking (Zappa *et al.* 2001), and spray and bubbles (Woolf 1993, 1997).

The air-sea exchange of heat (ie atmospheric stability) also influence CO_2 transfer. In Erickson (1993) it was shown that atmospheric stability alters the transfer velocity of CO_2 by between 20 and 50% due to the impact of stratification on the atmospheric gradients of wind speed and CO_2. In Rutgersson and Smedman (2010) the impact was, however, minor except for very low winds.

Zülicke (2005) formulated a theoretical framework for the variation of gas transfer due to molecular heat conduction; molecular heat conduction was estimated to have a significant impact below 1-2 m s^{-1}, with transfer velocity increasing under unstable and decreasing under stable atmospheric stratification conditions. Liss *et al.* (1981) found no significant enhancement due to evaporation in a tank experiment with limited water depth.

Water-side convection is generated by cooling at the surface caused by heat loss due to heat transport and evaporation. In addition to the heat loss evaporation also increases the surface salinity, which enhances the convection. When wind is in the low to intermediate speed regime convection is important for the mixing. For intermediate to higher winds the stress-induced mixing is typically dominating. The cooling of the surface leads to denser surface water and a circulation due to buoyancy, it generates large enough disturbance to the molecular diffusion layer to significantly enhance the transfer (Rutgersson and Smedman 2010; Rutgersson *et al.* 2011). Using data from the GasEx-2001 experiment, McGillis *et al.* (2004) demonstrated that CO_2 flux had a strong diurnal cycle and relatively high transfer velocity values; this was mainly explained by convection in the aquatic boundary layer. McGillis *et al.* (2004) suggested that traditional parameterization based on wind speed would underestimate gas flux by a factor of two in tropical regions due to ocean convection. Convective mixing increases the vertical transport of dissolved CO_2 in the mixed layer and leads to enhanced turbulence at the interface (Eugster *et al.* 2003).

In Rutgersson and Smedman (2010) the depth of the mixed layer during convective conditions was shown to be a controlling parameter and the characteristic velocity scale determined by the depth of the mixed layer and the strength of the buoyancy. Also other large scale eddy circulation systems in the

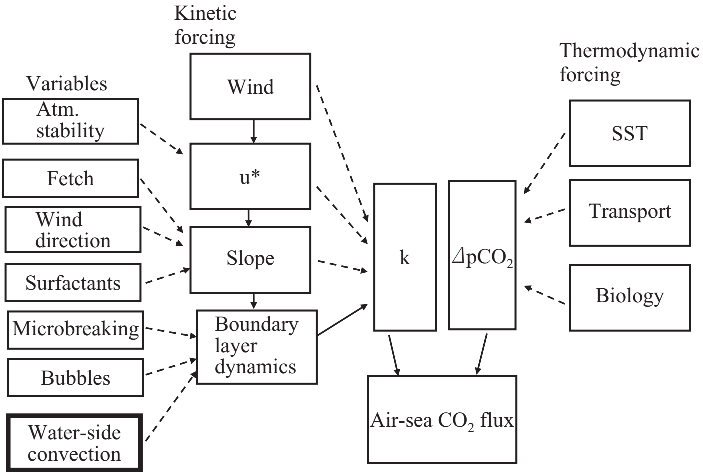

Figure 1 Simplified schematic (redrawn from Wanninkhof *et al.* (2009), with water-side convection added) of factors influencing air-sea CO_2 fluxes. On the right are factors that afffect the air-sea pCO_2 difference (thermodynamic forcing). On the left are environmental forcing factors that controll the efficiency of the transfer (kinetic forcing).

mixed layer could influence the transfer. One example of large eddy mixing is the Langmuir circulation (e.g. Sullivan and McWilliams, 2010).

Figure 1 is redrawn from Wanninkhof *et al.* (2009) and summarizes the environmental factors that influence the exchange. The water-side convection is here added, as it is one additional variable that influences boundary layer dynamics and has a potentially strong impact on the transfer velocity.

We here demonstrate the importance of water-side convection for the transfer velocity, in addition we evaluate three methods to introduce this effect when determining the transfer velocity and calculating the air-sea exchange. The methods all use the convective velocity and include (i) using a traditional wind-speed dependent transfer velocity, (ii) expressing waterside convection in a similar fashion as convectively driven gustiness in the atmosphere and (iii) using the concept of resistance, with waterside convection acting in parallel with other processes in the molecular sublayer.

2. Measurements

2.1 Site and instrumentation

The measurements are taken at the Östergarnsholm site in the Baltic Sea. This station is located at 57° 27′N, 18° 59′E, where a land-based 30-m tower situated on the southern tip of a very small, flat island.

The tower is equipped with high-frequency instrumentation for the turbulence measurements and slow-response sensors for mean profile measurements. High-frequency wind components are measured with SOLENT 1012R2 sonic anemometers (Gill Instruments, Lymington, UK) at three levels, i.e., 9, 16.5, and 25 m above the tower base. The humidity and CO_2 fluctuations are measured with a LICOR-7500 (LICOR-Inc., Lincoln, NE, USA) open-path analyzer at 9 m above the tower base.

For pCO_2^w and sea surface temperature (SST) a SAMI sensor (Sunburst Sensors, Missoula, MO, USA) is used (DeGrandpre *et al.* 2005). It is deployed at a depth of approximately 4 m, 1 km SE of the tower. The air-sea difference in partial pressure, ΔpCO_2 (where $\Delta pCO_2 = pCO_2^a - pCO_2^w$), is relatively large (of the order of 50-200 μatm) and positive for all data used in the following analysis. The measurement and instrumentation protocols are further described in Rutgersson *et al.* (2008; 2009).

Mixed layer depth was determined from a three-dimensional ocean model for the Baltic Sea (Funkqvist and Kleine 2007) as is described in Rutgersson and Smedman (2010).

3. Theory

3.1 Eddy correlation fluxes

The CO_2 air-sea flux on the tower is measured using the eddy-correlation technique, widely used to measure the flux of momentum, heat, and humidity. This method directly measures the amount and direction of the flux of the constituent (in this case CO_2) between the surface and the atmosphere. The correlation between simultaneously measured high-frequency fluctuations (of the order of 5-20 Hz) of vertical wind, w_a, and CO_2, c, gives the flux, F, in the atmosphere. The instrumental uncertainty in the measured flux ($\overline{w_a c'}$) was estimated to be approximately 17%, the mean uncertainty in the transfer velocity calculated from measurements is estimated to be slightly below 20% (Rutgersson *et al.* 2008). This estimated uncertainty reflects the instrumental errors and not potential methodological biases.

3.2 Calculated fluxes

The air-sea exchange of CO_2 is calculated from the air-sea difference in partial pressure of CO_2 at the surface and the gas transfer velocity (k) using the following equation (Wanninkhof 1992; Donelan and Wanninkhof 2002):

$$F=kK_0\Delta pCO_2=k_{660}\sqrt{\frac{660}{Sc}}K_0\Delta pCO_2 \tag{1}$$

where K_0 is the salinity- and temperature-dependent CO_2 solubility constant (K_0 is calculated using the empirical formulation from Weiss, 1974) and k is the transfer velocity of the exchange. The transfer velocity is usually considered to depend on wind speed, and also on the Schmidt number (Sc) (Jähne and Haussecker, 1998).

The buoyancy of the water (B) is the relevant parameter when determining the convection in the water. The water-side buoyancy is a function of the surface cooling (i.e., net heat flux) and of the evaporation, giving a more saline surface and thus enhancing the buoyancy. The water-side buoyancy flux is defined according to Jeffery *et al.* (2007):

$$B=\frac{gaQ_{net}}{c_{pw}\rho_w}+\frac{g\beta_{sal}Q_{lat}}{\lambda\rho_w} \tag{2}$$

where a is the thermal expansion coefficient, Q_{net} is the net surface heat flux (i.e., sensible and latent heat flux plus net long-wave radiation), c_{pw} is specific heat of water, ρ_w is the density of water, β_{sal} is the saline expansion coefficient, Q_{lat} is the latent heat flux, and λ is the latent heat of vaporization. Following atmospheric mixed-layer scaling, we define the water-side convective velocity scale as follows (MacIntyre *et al.* 2002; Jeffery *et al.* 2007):

$$w_*=(Bz_{ml})^{1/3} \tag{3}$$

where w_* indicates the strength of the water-side convection and z_{ml} the depth of the mixed layer. Stronger convective conditions (a larger value of B) and a deeper mixed layer (a larger value of z_{ml}) then produce stronger convective forcing in the water.

3.3 Modified NOAA-COARE gas transfer parameterization

The NOAA-COARE (National Oceanic and Atmospheric Administration-Coupled-Ocean Atmosphere Response Experiment) gas transfer parameterization incorporates several physical processes and is well suited for detailed estimates of air-sea CO_2 exchange, as well as for other gases (Fairall *et al.* 2000). It has been modified to include enhanced gas transfer due to bubbles (Woolf 1997), and buoyancy-driven transfer (Jeffery *et al.* 2007). In Jeffery *et al.* (2007) both sub-layer effects of buoyancy and convective mixing were introduced. The parameterization requires specification of a number of empirical coefficients, which can be fitted using field measurements. The gas transfer parameterization considers resistance to transfer in air and water, and includes both molecular and turbulent components:

$$k=\frac{u_{*a}}{\left(\sqrt{\frac{\rho_w}{\rho_a}}r_w\right)+r_a\alpha} \tag{4}$$

where u_{*a} is the atmospheric friction velocity, r_a resistance in the atmosphere, r_w resistance in the water, α the dimensionless solulubility and ρ_a air density. The convection in the ocean is introduced in a similar way as the convection in the atmosphere. In the atmosphere a gustiness parameter is used, which prevents the transfer velocity to approach zero at low winds. The average wind speed is expressed as a function of the vector wind and the convective velocity scale, (originally from Godfrey and Beljaars 1991).

In Jeffery *et al.* (2007) it is suggested that convection in the ocean is expressed in a similar fashion as in the atmosphere. The water-side convective addition (w_{gw}) to the velocity is calculated using the convective velocity scale:

$$w_{gw}=\beta w_* \tag{5}$$

where the empirical coefficient β was set equal to 1.

This is introduced in the NOAA-COARE algorithm by rewriting Equation 4 as

$$k=\left(\frac{r_w}{u_{*w}}+\frac{r_a a}{u_{*a}}\right)^{-1} \tag{6}$$

where u_{*w} is the friction velocity in the water. Then the waterside friction velocity is calculated as a function of waterside drag and water velocity (see Jeffery *et al.* (2007) for details).

3.4 Use water-side convection with concept of resistances

In Section 3.3 the impact of water-side convection is calculated similar as the enhancement of air-sea exchange of heat and water due to free convection in the atmosphere. There are, however, significant differences between these two processes. In the air the additional convection is added to represent velocity of the air during conditions when we have zero mean vector wind. In the water we introduce an additional process disturbing molecular diffusion layer and, in practice, adds a resistance to the transfer in the molecular diffusion layer in parallel with other processes.

Figure 2 shows a sketch including the different processes disturbing the molecular diffusion layer and then acts as resistances in parallel following the reasoning with an electric circuit. Here the total resistance is expressed as:

$$\frac{1}{r_w}=\frac{1}{r_U}+\frac{1}{r_B}+\frac{1}{r_{wc}}+\frac{1}{r_l} \tag{7}$$

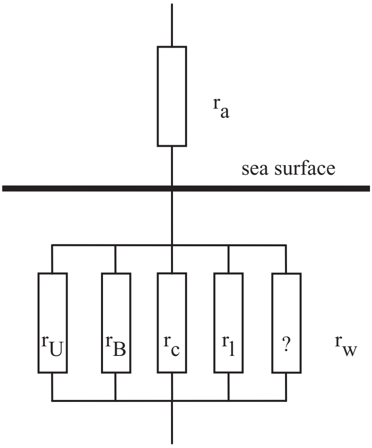

Figure 2 Schematic representation of processes acting in parallel to disturb the molecular sublayer in the water. The questionmark represent processes presently not described.

where r_U is the resistance due to shear generated diffusion, r_B is due to bubbles, r_{wc} is due to waterside convection, r_l is the potential impact of the Langmuir circulation. Also other possible processes can be added in Equation 7. The velocities are related to resistances as:

$$k_x = \frac{1}{r_x} \tag{8}$$

where $x = U, B, wc, l$, this means that

$$k_w = k_U + k_B + k_{wc} + k_l \tag{9}$$

k_w the total transfer velocity by the molecular diffusion.

The addition due to water-side convection is here expressed by Equation 10, since the addition due to convection is more dominant when the turbulence generated by shear (u_{*w}) is less.

$$k_{wc} = \gamma \sqrt{\frac{w_*}{u_{*w}}} \tag{10}$$

γ is an empirical coefficient. Using resistances to express water-side convection in the NOAA-COARE algorithm avoids the problem of having to define a velocity of the water at some reference depth and the water-side roughness length, which are not commonly used concepts in the ocean (Fairall *et al.* 2000). This is one drawback of the modified NOAA-COARE algorithm described in Section 3.3.

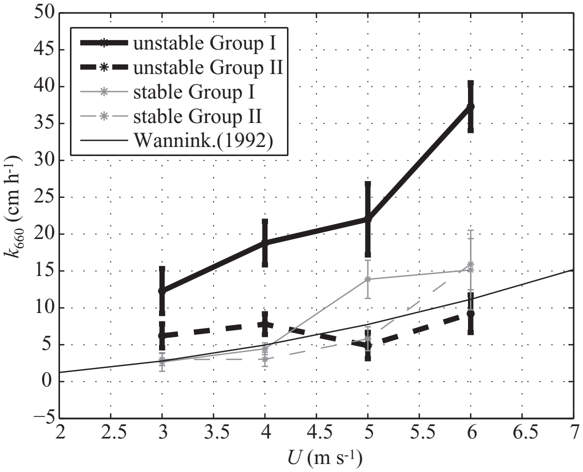

Figure 3 Averages of transfer velocity from measurements for wind speed intervals (3, 4, 5, 6 ± 0.5 ms^{-1}). Data are separated into Groups I and II (large and small mixed layer depths respectively) as well as into stable and unstable atmospheric stratification. Error bars represent ± one standard error of the mean. Thin solid line show transfer velocity from Wanninkhof (1992).

4. Results

The same data set as in Rutgersson and Smedman (2010) is used in the analysis. The data are divided into stable and unstable atmospheric stratification as well as two regimes: Group I, with a relatively large mixed layer depth (larger than 20 m); and Group II, when the mixed-layer depth is relatively small (less than 20 m). The following analysis includes data from March to July (for the three years used, 2005 to 2007).

Figure 3 shows the measured transfer velocity separated into Groups I and II and averaged over wind speed intervals. Stable and unstable conditions are treated separately.

For the unstable data (thick solid and dashed lines), the transfer velocities are significantly larger for Group I than for Group II. For stable data (thin solid and dashed lines), no such clear difference can be seen between the periods. The very large difference in the unstable data between Groups I and II points to the presence of an additional physical mechanism influencing the air-sea exchange. The major difference between the groups is in the depth of the mixed layer, so one can assume that for a period with a deep mixed layer (Group I) the air-sea transfer is significantly enhanced under convective conditions (here approximated with

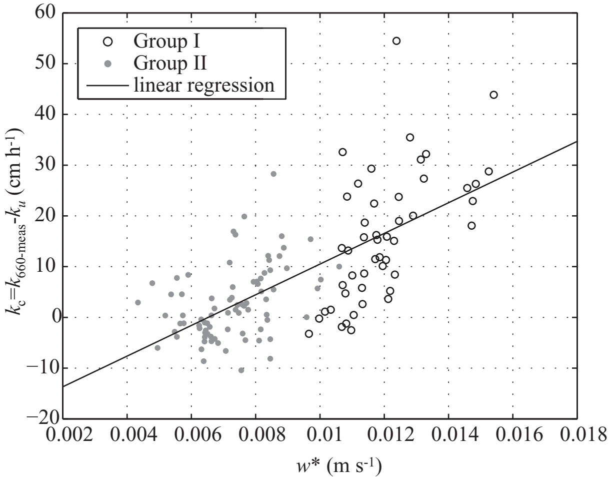

Figure 4 Contribution to total transfer velocity of the convection in the water. The solid line is the linear regression for both periods.

unstable atmospheric stratification); no such obvious enhancement is seen for non-convective conditions (i.e., stable atmospheric stratification).

4.1 Parameterizing water-side convection

The impact of water side convection on the transfer velocity can be introduced using Equation 11.

$$k = k_{660}\sqrt{\frac{660}{Sc}} = (k_u + k_c)\sqrt{\frac{660}{Sc}} \tag{11}$$

We assume that k_u describe the impact of all wind generated processes and correspond to the traditionally used parameterizations of k_{660}. The impact of the mixed layer convection (here k_c) is then added to the wind-speed dependent part. The magnitude of the convective forcing in the water-side mixed layer is described in terms of the convective velocity scale given by Equation 3. In Rutgersson and Smedman (2010) the threshold of mixed layer convective velocity to generate strong enough water-side convection is $w* = 0.006$. Using all data with only a minor contribution from water-side convection we can determine the wind-speed dependent part (Rutgersson and Smedman 2010):

$$k_u = 0.24U_{10}^2 \tag{12}$$

Then, k_c is estimated as the difference between the total measured transfer velocity, $k_{660-meas}$, and the wind-generated part (k_u given by Equation 12). Figure 4 shows $k_c = k_{660-meas} - k_u$ versus the convective velocity scale ($w*$); k_c increases relatively linearly with w_* and represents only the forcing of the waterside convection. Note that there is an addition from the convective velocity only when $w_* > 0.006$; below that point we assume that $k_c = 0$. Linear regression gives the equation:

$$k_c = 3022 w_* - 20 \tag{13}$$

which should only be used for positive values of k_c. The units used here are cm h^{-1} for k_c and m s^{-1} for w_*.

4.2 Introducing waterside convection in the NOAA-coare algorithm

When introducing the waterside convection in the NOAA-COARE algorithm (Sections 3.3 and 3.4) there are empirical coefficients to be determined. In Jeffery *et al.* (2007) the coefficient β in Equation 5 was selected to be $\beta = 1.0$, the enhancement of the transfer velocity was then between 0 and 1.4 cm h^{-1}. Using the data from the Östergarnsholm site (measured u_* and heat fluxes) to evaluate the modified NOAA-COARE algorithm (Section 3.3) with $\beta = 1.0$ the enhancement is of the order of 0.2 cm h^{-1}, which is too small compared to measured transfer velocity in this study. When instead using the modified NOAA-COARE algorithm (Section 3.3) and $\beta = 20$, the water-side convection data are of the same order of magnitude as the transfer velocity from the direct measurements (open circles in

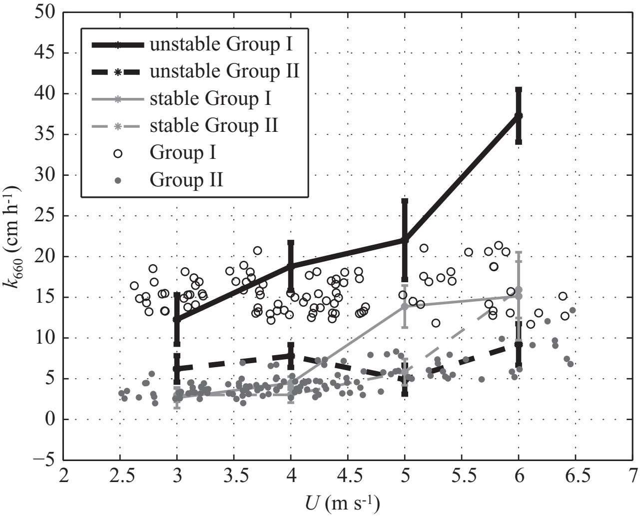

Figure 5 Solid and dashed lines according to Figure 3. Filled circles are transfer velocities calculated using the modified COARE algorithm (Section 3.3) for Group II data, open circles are for Group I data (when waterside convection is present and expressed using the concept of gustiness).

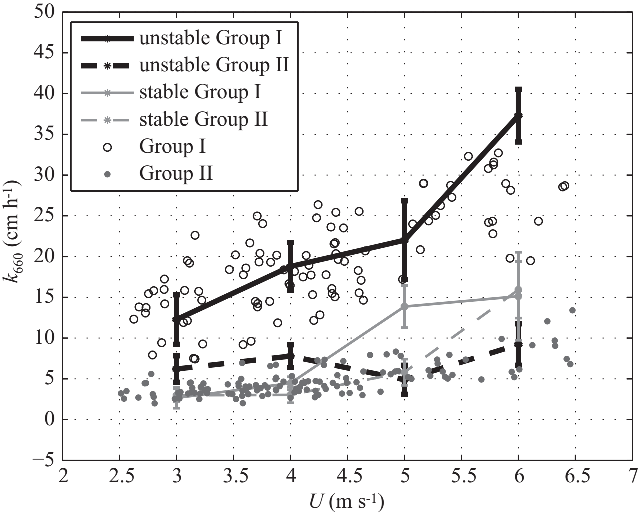

Figure 6 Solid and dashed lines according to Figure 3. Filled circles are transfer velocities calculated using the modified COARE algorithm (Section 3. 3) for Group II data, open circles are calculated using Equations 7 and 10) for Group I data (when waterside convection is present and expressed using the concept of resistance).

Figure 5 represent Group I data and unstable conditions). The increase with wind is, however, smaller than seen in measurements. Data with no water-side convection agrees well with measurements (filled circles in Figure 5).

When instead introducing waterside convection as an additional resistance acting in parallel with the impact of molecular diffusion and bubbles (in the framework of the NOAA-COARE algorithm as suggested by Equations 7 and 10) the agreement between calculated transfer velocity and transfer velocity from measurements is significantly improved. Figure 6 shows k_{660}, lines are from previous analysis, filled circles show k_{660} calculated using measured friction velocity and heat fluxes in the modified COARE-algorithm (Section 3.3) and represent Group II data and unstable conditions. Open circles represent calculated data (using Equations 7 and 10) and Group I data, waterside convection is thus included.

5. Discussion

Water-side convection is a previously mainly neglected air-sea exchange process. The waterside convection acts to enhance near surface turbulence and introduces motions, with a velocity scaling with the depth of the mixed layer. This induces a significant increase to the efficiency of the air-sea exchange as was also previously shown (MacIntyre *et al.* 2002; Eugster *et al.* 2003; McGillis *et al.* 2004). However, in previous studies the heating and cooling was due to the diurnal cycle by diurnal variation of the mixed layer depth and thus of water side convection. Using data from the Baltic Sea (from Rutgersson and Smedman, 2010), we do not have such a clear diurnal cycle, but a seasonal variation of the mixed layer depth induced by warming of the surface layer during spring and cooling during fall.

Introducing water-side convection when calculating transfer velocity can be done using different methods. Using the concept of resistances acting in parallel is appealing since it allows for introducing also other mechanisms presently not fully known. One such possible process is the Langmuir circulation, interacting with shear-induced turbulence as well as convective buoyancy in the water.

6. Summary and conclusions

Using data from the Östergarnsholm field station in the Baltic Sea, we can demonstrate that the CO_2 transfer velocity is significantly enhanced for a large portion of the data. Rutgersson and Smedman (2010) showed that this enhancement is most pronounced during unstable atmospheric stratification. It is likely that only molecular heat transport in the water-side molecular sub-layer is far too small to explain the large differences between the stable and unstable data. When separating the data into two regimes according to mixed-layer depth (i.e., large and small), there is a clear difference in transfer velocities between the two regimes (Groups I and II). For a large mixed-layer depth (more than 20 m), the transfer velocity is significantly enhanced, the degree of enhancement increasing as the surface cooling (buoyancy) increases. Using the convective velocity scale of the water (analogous to atmospheric convective scaling), the enhancement of the transfer velocity is clearly dependent on the water-side convective velocity.

The enhancement due to waterside convection can be added to the traditional transfer velocity expressed as $k_{660}=k_u+k_c$, where k_c here is expressed as $k_c=3022w-20$. Another method to introduce the enhancement due to waterside convection is to add an additional resistance in parallel with other processes acting to disturb the molecular sub layer. Here the resistance due to waterside convection is introduced in the NOAA-COARE algorithm as $k_{wc}=\gamma\sqrt{\frac{w*}{u*_w}}$.

Acknowledgements

Heidi Pettersson and the Aranda crew at FMI is thanked for helping mount the SAMI sensor.

References

DeGrandpre, M., T. Hammar, S. Smith, and F. Sayles (1995), In situ measurements of seawater pCO_2, *Limnol. Oceanog.*, *40*, 969-975.

Donelan, M., and R. ~Wanninkhof (2002), The critical importance of buoyancy flux for gas flux across the air-water interface, in *Gas Transfer at Water Surfaces*, edited by M. A. Donelan, W. M. Drennan, E. S. Saltzman, and R. Wanninkhof, pp. 1-10, Geophysical Monograph 127, American Geophysical Union.

Erickson III, D. (1993), A stability dependent theory for air-sea gas exchange, *J. Geophys. Res.*, *98*, 8471-8488.

Eugster, W., G. Kling, T. Jonas, J. P. McFadden, A. Wüest, S. MacIntyre, and F. S. Chapin (2003), CO_2 exchange between air and water in an Arctic Alaskan and midlatitude Swiss lake: Importance of convective mixing, *J. Geophys. Res.*, *108*, 4362.

Fairall, C. W., J. E. Hare, J. B. Edson, and W. R. McGillis (2000), Measurement and parameterization of air-sea gas transfer, *Boundary-Layer Meteorol*, *96*, 63-105.

Funkquist, L. and E. Kleine (2007), An introduction to HIROMB, an operational baroclinic model for the Baltic Sea, *Technical report*, *37*. SMHI, 601 76 Norrköping, Sweden.

Godfrey, J. S., and A. C. M. Beljaars (1991), On the turbulent fluxes of buoyancy, heat and moisture at the air-sea interface at low wind speeds, *J. Geophys. Res.*, *96*, 22043-22048.

IPCC (2007), Gas transfer at water surfaces - concepts and issues, Intergovernmental Panel on Climate Change's Synthesis Report. Climate Change.

Jähne, B., and H. Haussecker (1998), Air-water gas exchange, *Annual Review of Fluid Mechanics*, *30*, 443 - 468.

Jeffery, C., D. Woolf, I. Robinson, and C. Donlon (2007), One-dimensional modelling of convective CO_2 exchange in the tropical atlantic, *Ocean Modelling*, *19*(3-4), 161 - 182.

Liss, P., and L. Merlivat (1986), Air-sea gas exchange rates: Introduction and synthesis, in *The Role of Air-Sea Exchange in Geochemical Cycling*, edited by P. Buat-Menard, pp. 113-127, Reidel, Dordrecht.

Liss, P. S., B. W Balls, F. N. Martinelli, and M. Coantic (1981), The effect of evaporation and condensation on gas transfer across an air-water interface, *Oceanol. Acta*, *4*, 129 - 138.

MacIntyre, S., W. Eugster, and G. W. Kling (2002), The critical importance of buoyancy flux for gas flux across the air-water interface, in *Gas Transfer at Water Surfaces*, edited by M. A. Donelan, W. M. Drennan, E. S. Saltzman, and R. Wanninkhof, pp. 00-00, Geophysical Monograph 127, American Geophysical Union, Washington, DC.

McGillis, W. R., W. E. Asher, R. Wanninkhof, A. T. Jessup, and R. A. Feely (2004), Air-sea CO_2 exchange in the equatorial pacific, *J. Geophys. Res.*, *109*, C08S01.

Rutgersson, A., M. Norman, B. Schneider, H. Pettersson, and E. Sahlée (2008), The annual cycle of carbon dioxide and parameters influencing the airsea carbon exchange in the Baltic Proper, *J. Mar. Syst.*, *74*, 381-394.

Rutgersson, A., M. Norman, and G. Åström (2009), Atmospheric CO_2 variation over the Baltic Sea and the impact on air-sea exchange, *Boreal Env. Res.*, *14*, 238-249.

Rutgersson, A. and A. Smedman (2010), Enhancement of CO_2 transfer velocity due to water-side convection, *J. Mar. Syst.*, *80*, 125-134.

Siegenthaler, U., and J. Sarmiento (1993), Atmospheric carbon dioxide and the ocean, *Nature*, *365*, 119-125.

Sullivan, P. P., and J. C. McWilliams, (2010), Dynamics of Winds and Currents Coupled toSurface Waves, *Annual Review of Fluid Mechanics*, *42*, 19-42.

Takahashi, T., *et al.* (2002), Global sea-air CO_2 flux based on climatological surface ocean pCO_2, and seasonal biological and temperature effects, *Deep Sea Research*, *49*(9-10), 1601-1622.

Wanninkhof, R. (1992), Relationship between wind speed and gas exchange over the ocean, *J. Geophys. Res.*, *97*, 7373-7382.

Wanninkhof, R., W. E. Asher, and D. T. Ho, and C. Sweeney and W. R. McGillis (2009), Advances in QuantifyingAir-Sea Gas Exchange and Environmental Forcing, *Annu. Rev. Mar. Sci.*, *1*, 213-244.

Weiss, R. F. (1974), Carbon dioxide in water and seawater: the solubility of a non-ideal gas, *Mar. Chem.*, *2*, 203-215.

Woolf, D. (1993), Bubbles and the air-sea transfer velocity of gases, *Atmosphere-Ocean*, *31*, 517-540.

Woolf, D. (1997), Bubbles and their role in airsea gas exchange, in *The Sea Surface and Global Change*, edited by P. Liss and R. Duce, p. 173205, Cambridge University Press.

Zappa, C., W. Asher, and A. Jessup (2001), Microscale wave breaking and air-water gas transfer, *J. Geophys. Res.*, *106*, 9385-9391.

Zülicke, C. (2005), Air-sea fluxes including the effect of the molecular skin layer, *Deep Sea Research*, *52*, 1220-1245.